Elastic scattering, inelastic excitation, and neutron transfer for ^{7}Li + ^{120}Sn at energies around the Coulomb barrier

V. A. B. Zagatto and J. Lubian
Instituto de Física da Universidade Federal Fluminense, 24210-346, Niterói, Rio de Janeiro, Brazil

L. R. Gasques, M. A. G. Alvarez, L. C. Chamon, J. R. B. Oliveira, J. A. Alcántara-Núñez, N. H. Medina, V. Scarduelli, and A. Freitas
Instituto de Física da Universidade de São Paulo, 05508-090, São Paulo, São Paulo, Brazil

I. Padron
Centro de Aplicaciones Tecnológicas y Desarrollo Nuclear, 502, Calle 30, La Habana, Cuba

E. S. Rossi, Jr.
Centro Universitário Fundação Instituto de Ensino para Osasco, UNIFIEO, 06020-190, Osasco, São Paulo, Brazil

J. M. B. Shorto
Instituto de Pesquisas Energéticas e Nucleares, 05508-000, São Paulo, São Paulo, Brazil
(Received 12 May 2017; published 28 June 2017)

Experimental angular distributions for the ^{7}Li + ^{120}Sn elastic and inelastic (projectile and target excitations) scattering, and for the neutron stripping reaction, have been obtained at $E_{\rm LAB} = 20$, 22, 24, and 26 MeV, covering an energy range around the Coulomb barrier ($V_B^{\rm (LAB)} \approx 21.4$ MeV). Coupled channel and coupled reaction channel calculations were performed and both describe satisfactorily the experimental data sets. The $\frac{1}{2}^{-}$ state ^{7}Li inelastic excitation (using a rotational model), as well as the projectile coupling to the continuum (α plus a tritium particle) play a fundamental role on the proper description of elastic, inelastic, and transfer channels. Couplings to the one-neutron stripping channel do not significantly affect the theoretical elastic scattering angular distributions. The spectroscopic amplitudes of the transfer channel were obtained through a shell model calculation. The theoretical angular distributions for the one-neutron stripping reaction agreed with the experimental data.

DOI: 10.1103/PhysRevC.95.064614

I. INTRODUCTION

Scattering experiments have been used to characterize the mechanisms of the nuclear reactions and, from them, to obtain information about the structure of the nuclei. Some recent related works are, for instance, the measurement of the giant pair vibration process using transfer reactions [1], or the first observation of a nuclear structure without protons (resonant states generated by double charge exchange mechanisms) [2]. Also fundamental problems of physics (and nuclear physics) have been studied through nuclear reactions, as the nature of the neutrinos or the nuclear potential itself, as reported in Refs. [3] and [4], respectively. In particular, transfer reactions are an important tool to investigate the correlations between different nuclei and provide information about the corresponding structure. The nuclear structure affects the dynamics of the nuclear reaction, and therefore the structural parameters can be studied from the reactions.

Several works involving the ^{7}Li projectile reported the importance of the one-neutron stripping process [5–8]. This process presents significant cross sections, and it can be an intermediate step to breakup. The particular intensity of this reaction may be correlated to aspects of the nuclear structure of the lithium isotopes. To investigate such correlation, one should measure the neutron transfers in both ways, the ^{7}Li stripping (one of the objectives of the present work) and the ^{6}Li pickup channel (planned for the near future).

Weakly bound nuclei were present in the primordial nucleosynthesis and also contribute to stellar nuclear reactions, while exotic nuclei have major importance to astrophysical processes. Understanding the structure and reaction mechanisms involving weakly bound nuclei is a first step to understand the exotic nuclei [9,10]. The beam intensities for stable nuclei are higher than those for the exotic ones. Therefore, when measuring weakly bound nucleus reactions, larger statistics can be achieved and, consequently, more precise information about the corresponding reaction mechanisms can be obtained.

The current work complements our previous one [11], where the ^{120}Sn ($2^{+} \rightarrow 0^{+}$ transition) inelastic scattering was measured for ^{7}Li + ^{120}Sn in the same energy range. Using the particle-γ coincidence technique [12], it was not possible to measure cross sections for the elastic scattering and other nonelastic channels at the same time. The use of γ-ray detectors implies a low count rate and, as a consequence, channels with low cross sections were not properly observed.

Measurements for the ^{7}Li + ^{120}Sn system have been already reported in Refs. [13–15]. In the present work, the ^{7}Li + ^{120}Sn elastic scattering, the excitation of the 2^{+} and 3^{-} ^{120}Sn states, the projectile excitation to the first excited state, and the one neutron stripping reaction were all simultaneously measured at energies close to the Coulomb barrier ($V_B^{\rm (LAB)} \approx 21.4$ MeV). Nuclear structure spectroscopic

FIG. 1. View of the scattering chamber.

amplitudes obtained by means of shell model calculations were assumed in the nuclear reaction calculations, and the theoretical cross sections were compared to the experimental ones. Different types of calculations, concerning nuclear reactions and structure, were performed with the aim of studying the details of the reaction mechanisms and the interplay among them.

In the next section, we present a description of the experimental setup. In Sec. III, we present the theoretical framework adopted for the reaction and nuclear structure calculations. In the same section, the theoretical cross sections are compared with the experimental data. Finally, we present our main conclusions in Sec. IV.

II. EXPERIMENTAL SETUP

The ^{7}Li beam was delivered by the pelletron tandem accelerator, situated at the Open Laboratory of Nuclear Physics (LAFN, acronym in Portuguese) of the University of São Paulo. The bombarding energies were $E_{\mathrm{LAB}} = 20$, 22, 24, and 26 MeV. Data were taken in two consecutive experimental campaigns (the first for 20 and 24 MeV; the second for 22 and 26 MeV). The averaged beam intensity on the target was about 100 nA. Lower and higher intensities were used for measurements at forward and backward angles, respectively. The ^{7}Li beam was extracted from a lithium hydroxide cathode placed at the SNICS ion source. The target consisted of a thin foil of ^{120}Sn isotopically enriched (above 99%), with a thickness of 100 μg/cm^2, combined with an evaporated ^{197}Au backing layer used for normalization purposes.

Figure 1 presents the scattering chamber and the experimental setup. A tungsten collimator system is placed at the entrance of the chamber, in order to focus the beam on target. The target holder is placed at the center of the chamber. Surrounding the target holder, a set of nine surface barrier Si detectors is mounted. This detecting system allows the measurement over a 40° angular range, with 5° of angular step size. The detecting system is mounted on a rotating wheel (see Fig. 1), which allows us to change the detector angular positions without breaking the vacuum.

A typical spectrum of the experiment, for $\theta_{\mathrm{LAB}} = 125°$ and $E_{\mathrm{LAB}} = 24$ MeV, is presented in Fig. 2. To test the reproducibility of the experimental data, an overlap of one

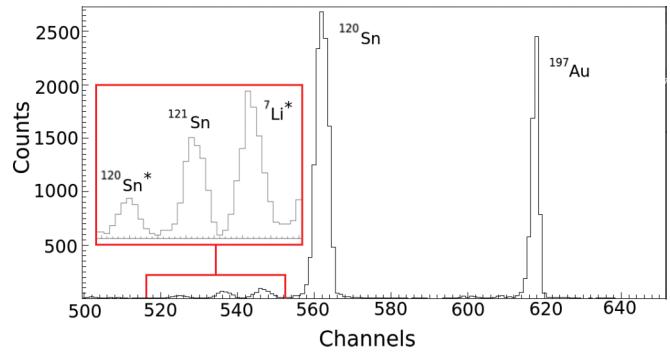

FIG. 2. Spectrum obtained for $\theta_{\mathrm{LAB}} = 125°$ at 24 MeV. The peaks corresponding to the elastic scattering of ^{7}Li on ^{120}Sn and ^{197}Au are indicated in the figure. The peaks corresponding to the 2^{+} ^{120}Sn excited state, the projectile excitation, and the one neutron stripping transfer are amplified in the inset.

or two angular positions was set for consecutive runs. Due to the corresponding large cross sections, the energy calibration of each detector was performed using the elastic peaks of the scattering on ^{120}Sn and ^{197}Au.

III. THEORETICAL CALCULATIONS AND DATA ANALYSIS

The theoretical calculations were performed with two different codes. The FRESCO code [16] was used to calculate the angular distributions within the coupled-channel formalism. NUSHELLX [17], a shell model code, was used to calculate the wave functions of the ^{120,121}Sn states and obtain the spectroscopic amplitudes necessary to calculate the one-neutron stripping reaction.

Different approaches have been adopted in our theoretical calculations. The simplest one corresponds to single-channel (elastic scattering) optical model calculations. After that, different sets of reaction channels were explicitly included in the coupled channel (CC) calculations: (i) the one-phonon 2^{+} and 3^{-} inelastic target excitations, (ii) the same channels of (i) plus the first excited state of ^{7}Li, and (iii) only the couplings to the ^{7}Li continuum (CDCC).

A typical CDCC calculation demands a high computational capacity. Thus, performing a complete calculation including the continuum plus the inelastic states and the transfer channels is prohibitive. An alternative way to simulate the effect of the breakup, assumed in the present work and named CC-TELP, consists in obtaining the trivially equivalent local polarization potential (TELP) from the CDCC calculations [18]. Subsequently, this polarization potential is included in the CDCC calculations. The validity of using the TELP to account for the effect of the breakup channels has been reported in Refs. [19,20]. Finally, the one-neutron transfer channel is included in the coupling scheme, added to the inelastic channels and TELP. We refer to this complete coupled reaction channel calculations as CRC.

A. The elastic channel

In our calculations, the double-folding São Paulo potential (SPP) [21–23] is used for the real part of the nuclear

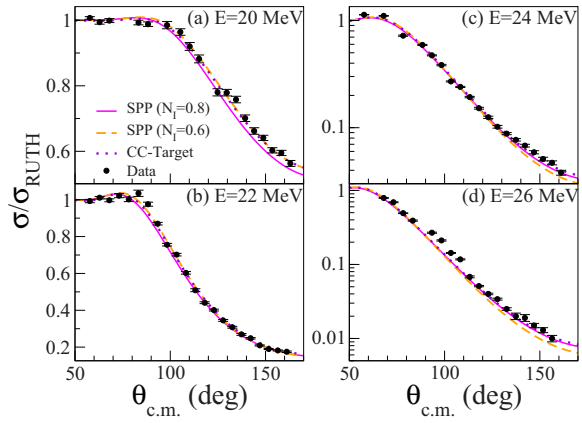

FIG. 3. Experimental and theoretical elastic scattering angular distributions for ^{7}Li + ^{120}Sn at bombarding energies of (a) 20, (b) 22, (c) 24, and (d) 26 MeV. See text for details.

interaction. For the imaginary part, the SPP is also assumed, but multiplied by a normalization factor N_I. A similar procedure was adopted in several other works. For instance, in Ref. [24] the analyses of elastic scattering data for several systems in a wide energy range resulted in N_I values around 0.8. The results of single-channel calculations with $(1 + 0.8i)\, V_{\rm SPP}(R)$ as the optical potential are represented in Fig. 3 by the solid magenta curves. In this approach, a slightly smaller $N_I = 0.6$ value provides a better data description for $E_{\rm LAB} = 20$ MeV (see the dashed yellow curves in the figure).

Despite of the good agreement between data and single-channel SPP results, the couplings to reaction channels are relevant for the elastic process at energies near the Coulomb barrier. The effect of these couplings does not appear in Fig. 3 because there is a partial compensation, since in the present case some couplings can produce attractive dynamic polarizations (inelastic and transfer) while others produce repulsive polarizations (breakup). Similar behavior has been recently reported for ^{8}B + ^{58}Ni [25].

B. Inelastic channels of ^{120}Sn

The ^{120}Sn inelastic coupled states are the 2^+_1 ($E^* = 1.171$ MeV), the triplet 0^+_2 ($E^* = 1.875$ MeV), 2^+_2 ($E^* = 2.097$ MeV), and 4^+_1 ($E^* = 2.194$ MeV) quadrupole states and the 3^-_1 ($E^* = 2.400$ MeV) octupole state. These states where coupled within the context of the vibrational model. It was observed, however, that the two-phonon triplet states have very small cross sections, which are compatible with our spectra, and these couplings practically do not affect the angular distributions of the other channels.

For the Coulomb transition amplitudes, $B(E2)\uparrow$ and $B(E3)\uparrow$, of the 2^+_1 and 3^-_1 states, we have assumed the same values as reported in Refs. [26–28] (see Table I). The corresponding deformation parameters δ_λ were obtained by considering the effect of the finite diffuseness value of the nuclear density, as discussed in Ref. [29]. This effect decreases the δ_λ values in comparison with those obtained from the sharp cutoff model. In fact, in the recent Ref. [15], where data for the same system have been obtained at energies slightly higher than those of the present work, the corresponding results for the deformation parameters are compatible with this effect.

TABLE I. Spin, excitation energies (MeV), transition amplitudes (e^2 b$^\lambda$) (from the g.s. to the excited states), and deformation lengths (fm) for the states included in our coupled channel calculations.

Nucleus	Spin	E^*	$B(E\lambda)$	δ_λ	Reference
^{120}Sn	2^+	1.171	0.25	0.80	[26,27]
^{120}Sn	3^-	2.400	0.12	0.76	[28]
^{7}Li	$1/2^-$	0.478	7.59	2.77	[30]

The CC calculations involving the target inelastic states (named CC-Target) were performed assuming the SPP optical potential with $N_I = 0.6$. The corresponding results for the cross sections are shown as violet dotted curves in Figs. 3 (elastic scattering), 4 (2^+_1 state), and 5 (3^-_1 state).

These couplings improve the description of the experimental elastic scattering angular distributions in comparison with the corresponding single-channel calculations. The experimental angular distributions for the 2^+ state are well described by the CC-Target calculations, except for the lowest bombarding energy, where some overestimation is observed at forward angles. It is possible that the coupling to the Coulomb breakup of ^{7}Li is stronger at this energy, removing some flux from the inelastic, but further investigations are necessary for a definite conclusion. At $E_{\rm Lab} = 20$ MeV, the theoretical 3^- inelastic excitation cross sections are very small. In fact, we were not able to measure them in our experiment. For the other energies, the agreement of the CC-Target theoretical results with the experimental data is quite good. A characteristic of the 3^- angular distributions is the dominance of the nuclear over the Coulomb excitations, since the calculated and measured cross sections are relevant only at the backward angles.

C. Inelastic channel of ^{7}Li

The ^{7}Li is a weakly bound nucleus with a breakup threshold of 2.45 MeV into α + tritium (corresponding to the main breakup mechanism). It has only one bound excited state: $1/2^-$ ($E^* = 0.478$ MeV). The coupling to the ^{7}Li excited state has been considered in the context of the rotational model, where we have assumed the $B(E2)\uparrow$ value from Ref. [30]. Once again, the effect of the finite diffuseness value of the nuclear density was considered for the determination of the deformation length (see Table I). This effect is quite large for light nuclei. We point out that such correction is crucial to obtain a good data description through the CRC calculations discussed ahead. Due to the very large deformation parameter of the ^{7}Li, we have assumed an option in the FRESCO code to guarantee the volume conservation to second order. Again, we have verified that the effect of this further correction is quite significant.

The CC cross sections, including both projectile and target inelastic excitations, are represented by green double-dot-dashed lines in Figs. 4 to 7 and named CC-Targ+Proj. In these calculations, $N_I = 0.6$ was kept for the imaginary part of optical potential.

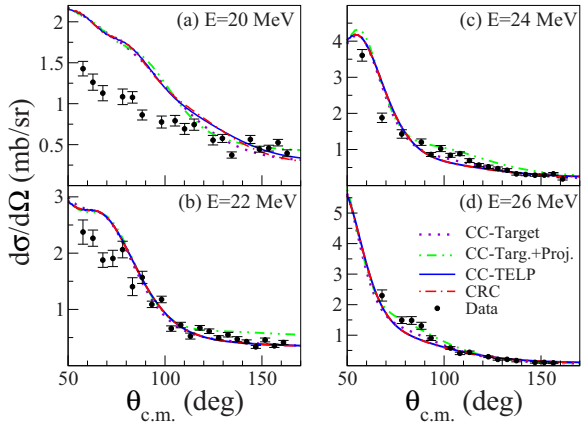

FIG. 4. Inelastic scattering angular distributions for the 2^+ state excitation of ^{120}Sn, at bombarding energies (a) 20, (b) 22, (c) 24, and (d) 26 MeV. See text for details.

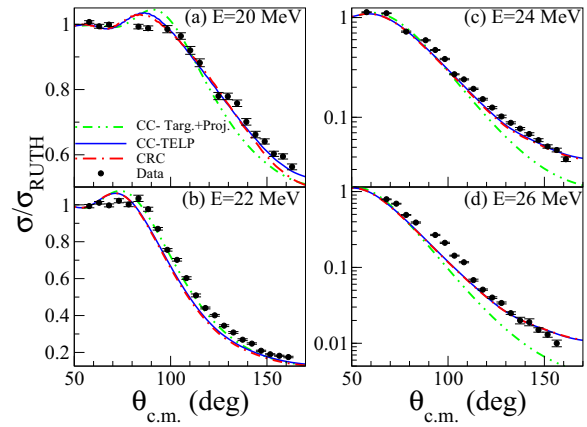

FIG. 6. Elastic scattering angular distributions for ^{7}Li + ^{120}Sn at bombarding energies of (a) 20, (b) 22, (c) 24, and (d) 26 MeV. Details of CC calculations can be found in the text.

These theoretical calculations provide a reasonable description of the experimental data for the ^{7}Li excitation (see Fig. 7). As shown in Fig. 4, the inclusion of the projectile excited state in the CC calculations significantly affects the cross sections for the 2_1^+ and 3_1^- ^{120}Sn excitations. A similar effect is observed concerning the elastic scattering process. In this case, the inclusion of the ^{7}Li inelastic coupling significantly worsens the description of the experimental data (compare the corresponding results in Figs. 3 and 6). In order to improve the agreement between theoretical and experimental cross sections, we tried to vary the N_I value. However, we were not able to obtain a good description simultaneously for all reaction processes with a unique N_I value for each energy. Therefore, other direct couplings should be included in the calculations to account for the data.

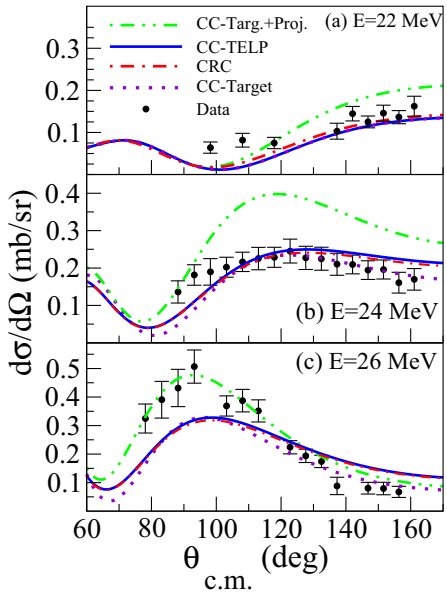

FIG. 5. Inelastic scattering angular distributions for the 3^- state excitation of ^{120}Sn, at bombarding energies (a) 22, (b) 24, and (c) 26 MeV. See text for details.

D. Coupling to continuum states of ^{7}Li

The inclusion of the continuum of ^{7}Li is usually performed by continuum discretized coupled channel (CDCC) calculations. The basic idea of the model is to describe the ^{7}Li as two cluster nucleus: an inert α particle core coupled to an inert tritium valence particle. It is then considered that all the excited states of the projectile are generated by the relative motion of the two clusters. It does not consider any other possible breakup channel of ^{7}Li (i.e., the ^{6}Li plus neutron breakup channel or subsequent decays of any particle). The continuum states of some energy intervals are grouped into wave packets with a defined angular momentum of the relative motion of the two clusters and they are usually denominated as bins. The wave functions of these bins belong to the Hilbert space, and consequently the matrix elements calculated with them have finite values. The other alternative method is to find a basis to expand the wave function. In the present work, we use the so-called bin method.

In the CDCC calculations performed in the present work, we have assumed the same bin parameters (i.e., bin width,

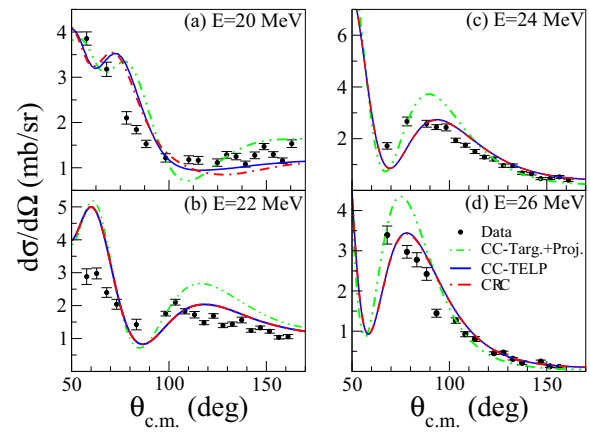

FIG. 7. Inelastic scattering angular distributions for the $1/2^-$ excited state of ^{7}Li at bombarding energies of (a) 20, (b) 22, (c) 24, and (d) 26 MeV. See text for details.

maximum bin energy, maximum relative α-tritium angular momentum) and optical potentials (α target and tritium target) used in Refs. [31] and [32], respectively. The potential used to account for the α-tritium interaction was the one from Ref. [33]. It has been shown that this interaction is able to describe the position of the ^{7}Li resonances as well as its width. It has been successfully used for the description of the breakup reaction of ^{7}Li with ^{59}Co [31], ^{144}Sm [34,35], ^{120}Sn [11]. Convergence of the calculations was achieved with 500 partial waves and a matching radius of 400 fm.

The CC calculations involving the inelastic excitations of the projectile and target, in which the TELP has been included in the optical potential, are called CC-TELP. The corresponding cross sections are represented by blue solid lines in Figs. 4 to 7. A good agreement with the data was obtained for the elastic and inelastic channels simultaneously. The N_I values obtained in these analyses are $N_I = 0.05$, 0.05, 0.10, and 0.25 for $E_{\mathrm{LAB}} = 20$, 22, 24, and 26 MeV, respectively. The differences of the CC-TELP and CC-Targ+Proj results indicate the importance of the coupling to the ^{7}Li continuum states

The strength of the imaginary part of the optical potential necessary to fit the data increases with the energy. This increase is necessary to properly account for the loss of flux of channels that are not explicitly coupled in the calculations. Therefore, small N_I values indicate that practically all the relevant channels are coupled, while large N_I suggests significant missing couplings. Some examples are the proton stripping process and the higher excited states of the one-neutron stripping process, measured for the same system at higher energies in Ref. [15].

E. One-neutron stripping

The theoretical calculations of the one-neutron stripping process involves two different aspects of nuclear theory. In order to obtain the spectroscopic amplitudes of the overlaps between states of the ^{120,121}Sn isotopes, a nuclear structure calculation has been performed. On the other hand, coupled reaction channel (CRC) calculations have been performed to obtain the cross sections of each state.

1. Nuclear structure calculations

The main difficulty in the nuclear structure calculations is to properly reproduce the order of the states of each nucleus, particularly those of the ^{121}Sn, which has an odd number of neutrons. It is important to remember that NUSHELLX performs a shell model calculation with some limitations, mainly when dealing with nuclei with intermediate and heavy masses, which is the case of the tin isotopes. For instance, the ^{120}Sn nucleus presents a well-known collective vibrational behavior for its low-lying excited states. Therefore, the shell model is not expected to adequately reproduce the energy levels of this nucleus.

When looking for spectroscopic amplitudes connecting states of different nuclei, it is necessary to describe these nuclei within the same model space. Thus, one should find a model space and interaction that satisfactorily describes both nuclei, using the same core nucleus. Therefore, to describe the ^{120,121}Sn nuclei, a lighter tin isotope may be used as a core.

The tin isotopes have always been of great interest for the nuclear structure researchers. Many attempts have been made to properly describe the characteristics of these isotopes, as shown in Refs. [36,37]. A common aspect of several attempts is that they succeeded in obtaining proper interactions that describe well the lighter (down to $A = 108$) and heavier (up to $A = 132$) tin isotopes. This is correlated to the fact that the magic numbers of the nuclear structure are located around these masses. Tin has a closed proton shell ($Z = 50$). For lighter isotopes, the neutron numbers are around the $N = 50$ closed shell, while for the heavier ones they are around the $N = 82$ closed shell. It has been a difficult task to find a proper interaction that describes the tin isotopes with intermediate masses, such as ^{120,121}Sn, since these nuclei have about half populated shell. For this reason, any structure calculation involves a large number of valence particles, which results in numerical calculations that demand a prohibitive time of computation.

The $SN100PN$ interaction [38] has been originally proposed to describe nuclei with mass number around $A = 132$ (specially the Sn, Te, and Xe isotopes), using a double magic core of ^{100}Sn. Although this interaction was not originally developed for this purpose, it has already been successfully used to describe nuclei with masses similar to those of the ^{120,121}Sn, using a constraint on the number of free nucleons of the lower shells [39].

Our calculations describe the nuclear structure of ^{120}Sn and ^{121}Sn simultaneously, including the $1g_{7/2}$, $2d_{5/2}$, $2d_{3/2}$, $3s_{1/2}$, and $1h_{11/2}$ orbitals and the $SN100PN$ interaction. Due to computational limitations, the following truncations were necessary in neutron orbits: The $1g_{7/2}$ was required to be full, at least 4 neutrons occupied the $2d_{5/2}$ orbit (similar results were obtained when considering a minimum of 2 neutrons), and the remaining neutrons were allowed to freely occupy the other orbits.

With these truncations, the excitation energy calculated for the 2_1^+ state of ^{120}Sn is 0.64 MeV, which is approximately half of the experimental value. This also happened with the triplet states. The results for the ^{121}Sn nucleus reproduced the $3/2^+$ as the ground state. An inversion occurred between the $11/2^-$ and $1/2^+$ excited states. As they are very close to each other (the difference in energy between them is only about 60 keV), their order is easily interchanged in calculations because their energy difference is lower than the usual accuracy of the shell model calculations (about 200 keV).

The spectroscopic amplitudes for the target overlaps ($< {}^{120}\mathrm{Sn}|{}^{121}\mathrm{Sn} >$) obtained from the shell model calculations are shown in Table II. In the shell model framework, the n, l, s, and j quantum numbers are related to the orbitals populated by the single neutron in the ^{120}Sn nucleus to construct the final states of the ^{121}Sn, and the spectroscopic amplitudes provide the strength of those overlaps. The spectroscopic amplitude information used for the calculation of the Lithium overlaps were taken from Ref. [40].

2. Coupled reaction channel calculations

In the CRC calculations, we have assumed the same N_I values as in the CC-TELP ones. For the final partition, the SPP

TABLE II. Spectroscopic amplitudes used in the CRC calculations. $n(ls)j$ are the quantum numbers of the neutron orbitals for the one-neutron transfer reaction.

^{120}Sn	^{121}Sn	nn	l	j	A_{lsj}
0^+	$3/2^+$	2	2	3/2	−0.633
0^+	$11/2^-$	1	5	11/2	0.393
0^+	$1/2^+$	3	0	1/2	−0.587
0^+	$3/2^+$	2	2	3/2	−0.205
2^+	$3/2^+$	3	0	1/2	−0.419
2^+	$3/2^+$	2	2	3/2	0.057
2^+	$11/2^-$	1	5	11/2	0.051
2^+	$1/2^+$	2	2	3/2	0.278
2^+	$1/2^+$	2	2	5/2	−0.312
2^+	$3/2^+$	3	0	1/2	0.474
2^+	$3/2^+$	2	2	3/2	−0.468

was also used for both real and imaginary parts of the optical potential, but with $N_I = 0.78$ (as proposed in the systematics of Ref. [24]). This procedure has been adopted because no couplings were considered in the final partition. The neutron-core nuclear interaction was described by a real Woods-Saxon potential (with reduced radius $r_0 = 1.2$ fm and diffuseness $a = 0.75$ fm) and with a spin-orbit term with the same geometrical parameters and fixed standard depth of 7.5 MeV. The depth of the central Woods-Saxon interaction was adjusted to reproduce the neutron-core experimental binding energy. The nonlocal kernels for single-particle finite range transfers were calculated using the prior representation with complex remnant.

The first ten states of ^{121}Sn were included in the CRC coupling scheme. For ^{6}Li only the ground state (g.s.) was considered. The spectroscopic amplitudes for the projectile overlaps were taken from Ref. [40]. The spectroscopic amplitudes for the target, obtained from the NUSHELLX calculations, are presented in Table II. Only the ground state and the $E^* = 0.006$, $E^* = 0.06$, and $E^* = 1.1$ MeV excited states presented relevant cross sections. Thus, in the final calculations, only these four states of ^{121}Sn have been included in the coupled scheme. Figure 8 shows a schematic representation of the CRC couplings, with the transitions considered between lithium and tin isotopes.

The theoretical cross sections obtained from the CRC calculations are shown as dot-dashed red lines in Figs. 4 to 7. These figures show that the couplings to the neutron transfer almost do not affect the cross sections for the elastic and inelastic channels.

The first excited state of ^{121}Sn has an excitation energy of only 6 keV. The difference between the energies of this state and the second excited one is about 54 keV. Therefore, the first three states (including the ground state) of this nucleus are compressed in a 60-keV region. Thus, it is very difficult to separate these states experimentally in our spectra. Therefore, the extracted areas of the spectra for neutron transfer represent the sum of the contributions of the first three ^{121}Sn states.

Figure 9 shows the angular distributions for the one-neutron stripping process. The theoretical contribution of the $3/2^+$ ^{121}Sn ground state is represented by the dashed green curves, while the dot-dashed orange and dotted blue curves

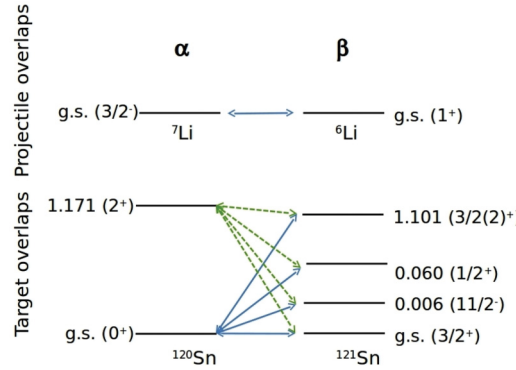

FIG. 8. Schematic representation of the CRC couplings. The solid blue lines represent the couplings between ground states of the initial partition (^{7}Li and ^{120}Sn) to the states of the final partition (^{6}Li and ^{121}Sn). The dashed green lines show the coupling of the ^{120}Sn excited state to ^{121}Sn states. The values of the excited state energies are given in MeV.

represent the $11/2^-$ and $1/2^+$ excited states, respectively. The solid red curves represent the sum of the cross sections for the three states. The data are very well reproduced by the theoretical calculations. This indicates that the spectroscopic amplitudes assumed for ^{6,7}Li and ^{120,121}Sn fit properly the data set.

We point out, however, that the theoretical transfer cross sections are rather dependent on the choice of the parameter values assumed for the neutron-core potential. For instance, a variation of 5% in the r_0 value for the radius of the projectile (from $r_0 = 1.20$ to 1.14 fm) results in a variation of about 6% in the transfer cross sections at $E_{\rm LAB} = 24$ MeV, while the same variation of r_0 for the target provides a transfer cross section change of ≈23%. Notwithstanding, the assumed spectroscopic amplitudes seem to be approximately right, since they fit the data well with $r_0 = 1.20$ fm. This value for the r_0 parameter

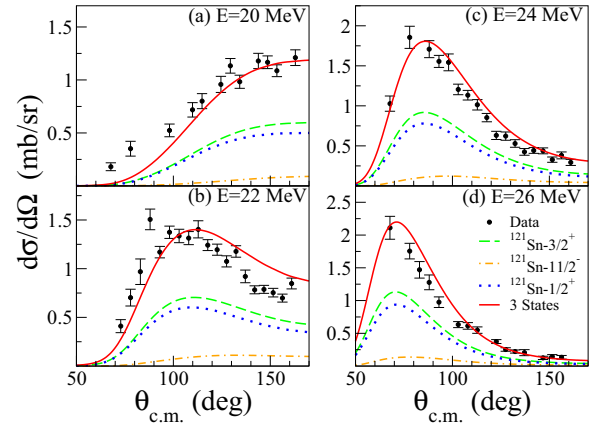

FIG. 9. Experimental and theoretical one-neutron stripping angular distributions. The contribution of the ^{121}Sn ground state is represented by the dashed green curve, the $11/2^-$ state corresponds to the dot-dashed orange curve, and the $1/2^+$ state is represented by the dotted blue curve. The solid red curve represents the sum of the cross sections of the three states.

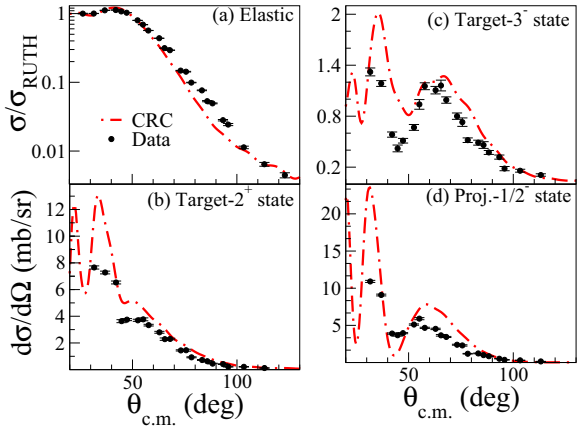

FIG. 10. Angular distributions: (a) elastic; (b) 2^+ and (c) 3^- states of ^{120}Sn; and (d) $1/2^-$ state of ^{7}Li. Data at 30 MeV from Ref. [15] are compared to CRC calculations performed in the present work.

is commonly adopted for nuclei with intermediate masses and no deformation, as the ^{120}Sn.

The CRC theoretical calculations performed in the present work have been extended to the analysis of the data at 28 and 30 MeV, recently reported in Ref. [15]. We have obtained a reasonable description of the cross sections for all channels (see Fig. 10 for the 30-MeV calculations). However, the data fit for both energies required a small $N_I = 0.05$ value. This behavior might be correlated to the difficulty of obtaining a well-converged CDCC calculation (to obtain the TELP) at these higher energies.

IV. CONCLUSIONS

In this work, we presented experimental angular distributions for several channels of the ^{7}Li + ^{120}Sn system at energies around the Coulomb barrier. Extensive theoretical calculations were performed, allowing the comparison of different approaches with the data.

The description of the elastic scattering through single-channel calculations was achieved with the standard São Paulo potential ($N_I = 0.8$). A good description is also obtained when coupling the target excitation channels (with $N_I = 0.6$), except at the lowest energy. Nevertheless, the inclusion of the ^{7}Li excited-state coupling strongly affects all the other channels and significantly worsens the data fit. On the other hand, the inclusion of the effect of the breakup, through the TELP, provides a good overall description of the data set. This is a clear indication of the importance of the couplings to the continuum.

Nuclear structure calculations were carried out to obtain spectroscopic amplitudes for the one-neutron stripping. The calculated quantities, spin, parity, order of levels, and their energies, were fairly compatible with the experimental values for the ^{120,121}Sn nuclei. The parameters obtained from these nuclear structure calculations were assumed in the CRC ones. The experimental angular distributions for the one-neutron transfer were well described by such CRC calculations. The one neutron transfer couplings do not affect the cross sections of the other channels. The agreement between data and theoretical calculations indicates that the spectroscopic amplitudes for ^{120,121}Sn obtained with NUSHELLX, as well as those for ^{6,7}Li provided by Ref. [40], are appropriate.

ACKNOWLEDGMENTS

This work was partially supported by FAPERJ, FAPESP, CAPES, and CNPq, Brazil. We would also like to thank Dr. Nemitala Added and the technical staff of LAFN for assisting in the maintenance and operation of the accelerator. We also thank Dr. A. M. Moro for fruitful discussions and Dr. A. Kundu for providing the data of Ref. [15].

[1] F. Cappuzzello, D. Carbone, M. Cavallaro, M. Bondi *et al.*, Nat. Commun. **6**, 6743 (2015).
[2] K. Kisamori, S. Shimoura, H. Miya, S. Michimasa *et al.*, Phys. Rev. Lett. **116**, 052501 (2016).
[3] F. Cappuzzello, M. Cavallaro, C. Agodi, M. Bondi, D. Carbone, A. Cunsolo, and A. Foti, Eur. Phys. J. A **51**, 145 (2015).
[4] J. R. B. de Oliveira, F. Cappuzzello, L. C. Chamon, D. Pereira *et al.*, J. Phys. G: Nucl. Part. Phys. **40**, 105101 (2013).
[5] N. J. Davis, R. P. Ward, K. Rusek, N. M. Clarke *et al.*, Phys. Rev. C **69**, 064605 (2004).
[6] Y. Tokimoto, H. Utsunomiya, T. Yamagata, M. Ohta, Y.-W. Lui, R. P. Schmitt, S. Typel, Y. Aoki, K. Ieki, and K. Katori, Phys. Rev. C **63**, 035801 (2001).
[7] D. H. Luong, M. Dasgupta, D. J. Hinde, R. du Rietz, R. Rafiei *et al.*, Phys. Lett. B **695**, 105 (2011).
[8] D. Martinez Heimann, A. J. Pacheco, O. A. Capurro, A. Arazi *et al.*, AIP Conf. Proc. **1423**, 109 (2012).
[9] J. P. Fernandez-Garcia, M. Cubero, L. Acosta, M. Alcorta *et al.*, Phys. Rev. C **92**, 044608 (2015).
[10] M. Cubero, J. P. Fernandez-Garcia, M. Rodriguez-Gallardo, L. Acosta *et al.*, Phys. Rev. Lett. **109**, 262701 (2012).
[11] V. A. B. Zagatto, J. R. B. de Oliveira, L. R. Gasques, J. Alcantara-Nunez *et al.*, J. Phys. G **43**, 055103 (2016).
[12] V. A. B. Zagatto, J. R. B. de Oliveira, P. R. P. Allegro, L. C. Chamon *et al.*, Nucl. Inst. Meth. A **749**, 19 (2014).
[13] K. Becker, K. Blatt, H. J. Jansch, W. Korsch *et al.*, Nucl. Phys. A **535**, 189 (1991).
[14] D. P. Sousa, D. Pereira, J. Lubian, L. C. Chamon *et al.*, Nucl. Phys. A **836**, 1 (2010).
[15] A. Kundu, S. Santra, A. Pal, D. Chattopadhyay, R. Tripathi, B. J. Roy, T. N. Nag, B. K. Nayak, A. Saxena, and S. Kailas, Phys. Rev. C **95**, 034615 (2017).
[16] I. J. Thompson, Comp. Phys. Rep. **7**, 167 (1988).
[17] B. A. Brown and W. D. M. Rae, Nucl. Data Sheets **120**, 115 (2014).
[18] I. J. Thompson, M. A. Nagarajan, J. S. Lilley, and M. J. Smithson, Nucl. Phys. A **505**, 84 (1989).
[19] J. Rangel, J. Lubian, L. F. Canto, and P. R. S. Gomes, Phys. Rev. C **93**, 054610 (2016).

[20] J. Lubian, and F. M. Nunes, J. Phys. G **34**, 513 (2007).
[21] M. A. Cândido Ribeiro, L. C. Chamon, D. Pereira, M. S. Hussein, and D. Galetti, Phys. Rev. Lett. **78**, 3270 (1997).
[22] L. C. Chamon, D. Pereira, M. S. Hussein, M. A. Candido Ribeiro, and D. Galetti, Phys. Rev. Lett. **79**, 5218 (1997).
[23] L. C. Chamon, B. V. Carlson, L. R. Gasques, D. Pereira, C. De Conti, M. A. G. Alvarez, M. S. Hussein, M. A. Candido Ribeiro, E. S. Rossi, Jr., and C. P. Silva, Phys. Rev. C **66**, 014610 (2002).
[24] M. A. G. Alvarez, L. C. Chamon, M. S. Hussein, D. Pereira *et al.*, Nuc. Phys. A **723**, 93 (2003).
[25] J. Lubian, T. Correa, P. R. S. Gomes, and L. F. Canto, Phys. Rev. C **78**, 064615 (2008).
[26] S. Raman, C. W. Nestor, and P. Tikkanen, At. Data Nucl. Data Tables **78**, 1 (2001).
[27] D. S. Andreev, V. D. Vasilev, G. M. Gusinskii, K. I. Erokhina, and I. K. Lemberg, Izvest. Akad. Nauk SSSR, Ser. Fiz. **832**, 25 (1961); Columbia Tech. Transl. **842**, 25 (1962).
[28] T. Kibédi and R. H. Spear, At. Data Nucl. Data Tables **80**, 35 (2002).
[29] L. C. Chamon and B. V. Carlson, Nucl. Phys. A **846**, 1 (2010).
[30] W. J. Vermeer, R. H. Spear, and F. C. Barker, Nucl. Phys. A **500**, 212 (1989).
[31] A. Diaz-Torres, I. J. Thompson, and C. Beck, Phys. Rev. C **68**, 044607 (2003).
[32] R. A. Broglia and A. Winther, in *Heavy-Ion Reactions, Parts I and II*, FIP Lecture Notes Series (Addison-Wesley, New York, 1991).
[33] A. Diaz-Torres and I. J. Thompson, Phys. Rev. C **65**, 024606 (2002).
[34] D. R. Otomar, J. Lubian, P. R. S. Gomes, T. Correa, J. Phys. G **40**, 125105 (2013).
[35] D. R. Otomar, J. Lubian, P. R. S. Gomes, D. S. Monteiro *et al.*, Phys. Rev. C. **80**, 034614 (2009).
[36] A. Holt, T. Engeland, M. Hjorth-Jensen, and E. Osnes, Nucl. Phys. A **34**, 41 (1998).
[37] F. Andreozzi, L. Coraggio, A. Covello, A. Gargano, T. T. S. Kuo, and A. Porrino, Phys. Rev. C **59**, 746 (1999).
[38] B. A. Brown, N. J. Stone, J. R. Stone, I. S. Towner, and M. Hjorth-Jensen, Phys. Rev. C **71**, 044317 (2005).
[39] D. S. Judson, A. M. Bruce, T. Kibédi, G. D. Dracoulis *et al.*, Phys. Rev. C **76**, 054306 (2007).
[40] S. Cohen and D. Kurath, Nucl. Phys. A **101**, 1 (1967).